NUCL SCI TECH (2016) 27:27
DOI 10.1007/s41365-016-0032-7

The behavior of HfB_2 under neutron irradiation

Mohammad Mehdi Nasseri[1]

Received: 12 April 2015 / Revised: 28 July 2015 / Accepted: 11 August 2015 / Published online: 6 April 2016

Abstract Due to the interesting properties of hafnium diboride (HfB_2) as a ceramic, it has drawn considerable attention from several researchers. To understand the radiation properties of HfB_2 that may be used in the nuclear industry, the interaction of this composite under neutron irradiation was studied. It is obvious that, because HfB_2 has Boron, this composite has the potential to absorb neutrons particularly in the range of thermal energy. The ^{10}B (n, α) ^{7}Li interaction is dominant among other interactions that produce alpha particles. The results revealed that alpha particles have a high fluctuation diagram following a saw-tooth spectrum for thermal neutron energy, which has to be carefully analyzed. If HfB_2 is intended to be used in fusion facilities, for example in fusion reactors, its interaction with high neutrons (14 MeV) should be studied. The results of this case showed that, in the wide range of alpha energy, the amount of alpha particles is almost constant, so this continuum spectrum is almost flat and there is just a small peak at 2.31 MeV that belongs to the very famous interaction [^{10}B (n, α) ^{7}Li].

Keywords HfB_2 · Geant4 · Thermal neutron · High-energy neutron · Alpha particle

✉ Mohammad Mehdi Nasseri
mnasseri@aeoi.org.ir

1 School of Plasma Physics and Nuclear Fusion, Institute of Nuclear Science and Technology (AEOI), Tehran 141551339, Iran

1 Introduction

High-efficiency materials in radiation environments and safety remarks in the nuclear industry have always been the concern of nuclear material scientists and necessitate them to introduce new materials. Each nuclear facility, even each part of it, requires particular materials to operate properly. One of the materials that was recently introduced is a kind of ultra-advance ceramic called HfB_2. HfB_2's elements, hafnium (Hf) and boron (B), have a high capacity to absorb neutrons [1–3]. The neutron thermal cross sections of stable Hf and B are 14 and 3980 Barns, respectively. Some HfB_2 properties are listed in Table 1.

These excellent thermal, mechanical and nuclear properties are the reasons for using HfB_2 as a control rod in fission power plant reactors (e.g., pressurized water reactors (PWRs)) [4]. Neutron calculation and measurement in fusion facilities like tokomak are very important [5, 6], and HfB_2 also may play an important role as the first wall of tokomaks.

Therefore, HfB_2 ceramic with all these properties would be a good candidate for such purposes. Despite these interesting properties, there are some difficulties in using HfB_2 under irradiation of neutrons. This issue originates from the nuclear interactions especially ^{10}B (n, α) ^{7}Li.

For example, through ^{10}B (n, α) ^{7}Li interaction, the ^{10}B isotope transforms into an ^{7}Li isotope plus an alpha particle. There are two modes of interaction as follows:

$$n + {}^{10}B \rightarrow {}^{7}Li^{*} + \alpha, Q = 2.31\,MeV + \gamma\,(0.48\,MeV)(93\,\%)$$

$$n + {}^{10}B \rightarrow {}^{7}Li + \alpha, Q = 2.78\ \ MeV(7\,\%).$$

Although these interactions are dominant, other interactions like:

Table 1 HfB_2 ceramic properties

Properties	Value
Molar mass (gr)	200.112
Melting temperature (°C)	3380
Density at 25 °C (g/cm^3)	11.2
Water solubility	Insoluble
Crystal structure	Hexagonal
Young's modulus (GPa)	480
Hardness (GPa)	28
Coefficient of thermal expansion (°C^{-1})	6.3×10^{-6}
Heat capacity at 25 °C (J mol^{-1} °C^{-1})	49.5
Thermal conductivity (W m^{-1} °C^{-1})	104

$$^{11}\mathrm{B}\ (\mathrm{n},\alpha)^{8}\mathrm{Li}(\beta^{-}) \rightarrow^{8} \mathrm{Be}^{*}(2\alpha) \quad \text{or}$$

$$^{178}\mathrm{Hf}(\mathrm{n},\ \alpha)^{175}\mathrm{Yb} \quad \text{or}$$

$$^{180}\mathrm{Hf}(\mathrm{n},\ \alpha)^{177}\mathrm{Yb},$$

may also happen. The emitted particle, which is basically ^4He, will be absorbed by the material and will cause defects and dislocation in HfB_2, which collapses its structure.

According to the literature, thermal neutrons produce alpha particles with an average energy of 1.48 MeV and a lithium ion with an average energy of 0.83 MeV [7]. The interaction of neutrons with HfB_2 also produces prompt γ rays which need more precautions when shielding is intended with this compound.

Several experiments have been carried out to determine the cross section of the ^{10}B (n, α) ^7Li interaction [8, 9]. Some investigators have compared the practical results with databases such as the Evaluated Nuclear Data Format (ENDF) or the Japanese Evaluated Nuclear Data Library (JENDL), in a limited energy range [10, 11].

In this study, the well-known Geant4 has been used to simulate the behavior of HfB_2 interactions with neutrons in a wide range of neutron energy. The high precision of Geant4 (HP) model covers the spectrum of 0–20 MeV neutron energy. In this range, the Geant4 Nuclear Data Library (G4NDL) matches the ENDF and JENDL. The model considers neutron interaction with matter, including capture, elastic, inelastic {(n, γ) (n, α), (n, 2n), (n, nα), (n, np}, and also different models for the ion interactions [12]. Geant4 has been used for several simulation purposes and shows its validity [13–17].

2 Virtual experiment

A rectangular bulk sample with surface area of 10 cm × 10 cm and thicknesses of 2, 10, 20, 50, and 100 mm has been selected for the simulation. The bulk sample was bombarded by a square neutron beam with the same surface area in a fixed distance of 10 cm from the surface of the bulk sample, as shown in Fig. 1. The sample surface was then hit by 10^6 neutrons during each virtual experiment.

Various simulations have been carried out with mono energy neutrons of 0.025 eV, 1 eV, 1 keV, 100 keV, 1 MeV, 10 MeV and 14 MeV to determine the alpha particles resulting from ^{10}B (n, α) ^7Li or other (n, α) interactions. Figure 2 depicts all interactions from a 100 mm thickness of HfB_2 slab, except 14 MeV neutrons. It was observed that, in the range of 0.025 eV–100 keV of neutron energies, the amount of alpha particle spectrums had a drastic fluctuation reaching 1.8 MeV. The compound did not produce any more alpha particles. In Fig. 2, the fluctuation is due to the alpha particle collisions. On the other hand, the fluctuation is due to counting all alpha particles, either produced or collided ones. As we know, when alpha particles collide with matter, it loses its energy in specific

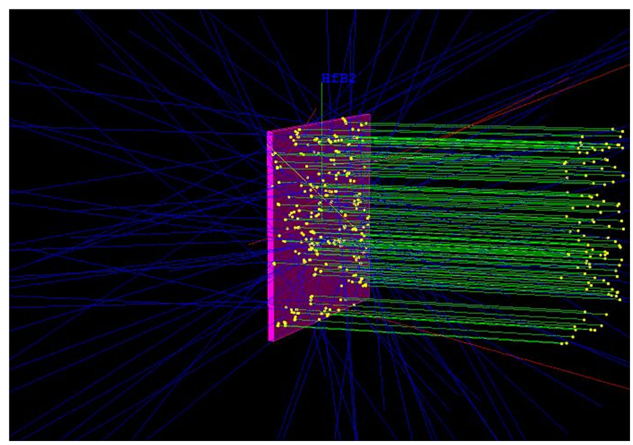

Fig. 1 Virtual experiment of irradiation of neutron on HfB_2

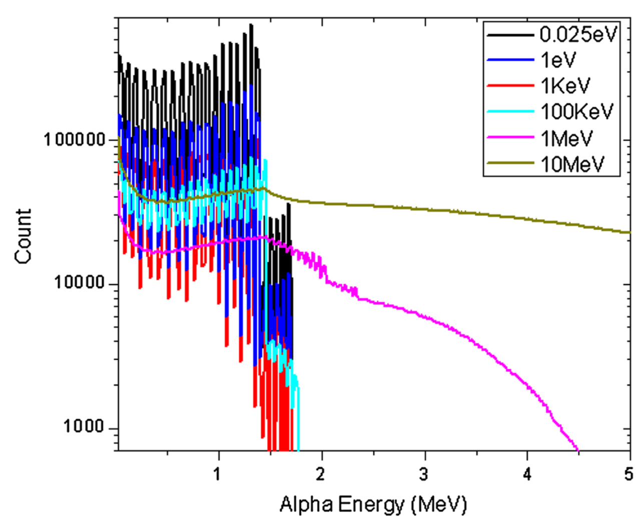

Fig. 2 Alpha particles spectrum in 100 mm thickness of HfB_2 as a result of all (n, α) interactions by different neutron energies

amounts, which means we have particles in discrete energy. So if we count all these particles, then we have such fluctuations in the spectrum. This spectrum shows the alpha particles that exist in the material at any moment of time. 10 MeV energy has been divided into 256 channels; therefore, with the discrete energy of alpha particles, we must have increased or decreased amounts in each channel. This fluctuation would be seen for high counting, especially in the logarithmic scale. If we notice the spectrum for 1 MeV or 10 MeV neutron energy, we can see that all the alpha particles are not enough so we do not have such fluctuation in those spectrums.

It was also recognized that, at 1 MeV neutrons, the alpha particles have an energy range of 0–4.5 MeV. 4.5 MeV alpha particle energy is not because of B (n, α) Li. These alphas could be created via other inelastic interactions of neutrons with matter. At 10 MeV of neutron energy, the amount of produced alpha particles changes to around 4 %, which indicates that only 4 % of the 10 MeV neutron flux has been involved in the (n, α) interaction to produce alpha particles. This amount then gradually decreases and ends before 8 MeV.

The general shape of the alpha particles spectrum is the same for different thicknesses of the HfB_2 slab. Figure 3 is plotted for 14 MeV neutron interactions with different thicknesses of HfB_2 slab. It indicates that thicker slabs produce more alpha particles. Figure 3 also reveals that the amount of lower energy alpha particles is higher with descending trends toward a 1.8 MeV alpha particle energy. At 1.8 MeV, a flat peak appears, then followed by a gradually continuing slope, and it suddenly drops at 7.4 MeV. After that, the alpha particles' energy ended at 8 MeV.

The interaction of neutrons with HfB_2 produces some amount of energy, which would be absorbed by the compound. The deposited energy, as part of a single neutron, was analyzed by different thicknesses of the HfB_2 slab, and

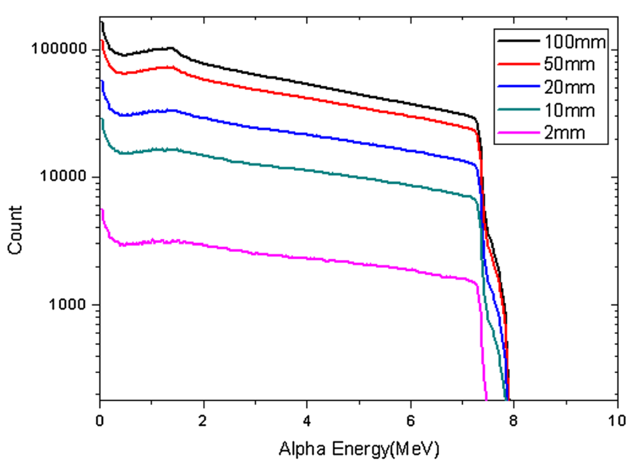

Fig. 3 Alpha particles spectrum produced in different thicknesses of HfB_2 as a result of all (n, α) interactions by 14 MeV neutron energy

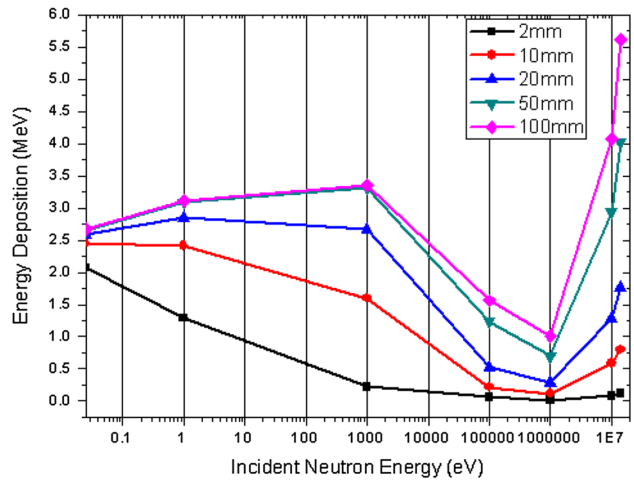

Fig. 4 Amount of energy deposition versus the energy of incident neutrons

the results are plotted in Fig. 4. As reported by some researchers [7], in ^{10}B (n, α) ^{7}Li interaction, the sum of the ^{4}He and ^{7}Li kinetic energies (0.83 + 1.48 MeV) is 2.31 MeV. The starting point in Fig. 4 shows that the 0.025 eV thermal neutrons produce 2.48 MeV on average, which closely agrees with the reported value.

Departing from the starting point, the deposited energy within the compound reduces and reaches its minimum value of around 0.2–0.5 MeV, followed by a rapid increase thereafter. The increase in deposited energy could be due to the multiplication of elastic interactions that may produce low-energy neutrons in conjunction with the repeating interaction of ^{10}B (n, α) ^{7}Li.

This phenomenon has been analyzed and depicted separately in Fig. 5. The figure shows that neutrons' elastic interactions start from 10 keV onward and boost swiftly as the energy of the neutrons becomes higher.

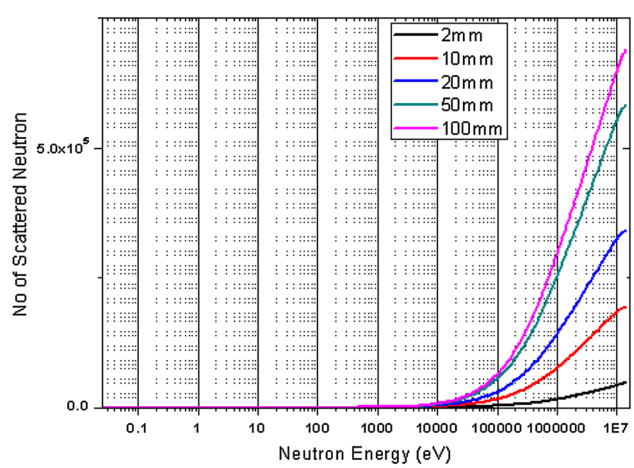

Fig. 5 Amount of scattered neutrons versus different neutron incident energies

3 Conclusion

The behavior of HfB_2 interaction with a wide energy range of neutrons was studied. Boron has a major influence on HfB_2 performance, and its large thermal neutron cross section plays the main role. Although Boron can absorb more neutrons, the ^{10}B (n, α) ^{7}Li interaction may introduce some defects in the HfB_2 structure. Based on this concept, the amount of produced alpha particles and deposited energy within the HfB_2 compound interacting with neutrons has been simulated. This virtual experiment approach is very helpful in inserting alpha detectors as well as neutron detectors in between the HfB_2 composite, which is very challenging and even impossible. Neutron irradiation to the HfB_2 composite affects the amount of Boron during this time. So, all computation of defective effects are time dependent for future studies.

Acknowledgments This work was supported by the School of Plasma Physics and Nuclear Fusion, Institute of Nuclear Science and Technology (AEOI). The authors would like to thank Dr. Mohammad Mehdi Farhoudi for his useful comments.

References

1. M.A. Misheva, G. Toumbev, Radiation defects in HfB2 after neutron irradiation studied by perturbed angular correlations of ^{181}Ta. Radiat. EFF Defects **90**, 57–66 (1985). doi:10.1080/00337578508222516
2. Z.F. Li, X.X. Xue, S.L. Liu et al., Effects of boron number per unit volume on the shielding properties of composites made with boron ores from China. Nucl. Sci. Tech. **23**, 344–348 (2012). doi:10.13538/j.1001-8042/nst.23.344-348
3. X.B. Yin, Y.Z. Wei, J.H. Zu, Adsorption behavior of Zr(IV) and Hf(IV) on a silica-based macroporous TODGA adsorbent. Nucl. Sci. Tech. **24**, 040203 (2013). doi:10.13538/j.1001-8042/nst.2013.04.009
4. P. Cheminant, X. Deschanels, L. Boulanger et al., Microstructural damage in hafnium diboride under neutron irradiation. Key Eng. Mat. **132**, 643–646 (1997). doi:10.4028/www.scientific.net/KEM.132-136.643
5. X.F. Jiang, J. Cao, C.Y. Jiang et al., Tokamak fusion neutron spectrometer based on PXI bus. Nucl. Sci. Tech. **25**, 040401 (2014). doi:10.13538/j.1001-8042/nst.25.040401
6. S.P. Li, X.F. Xu, H.R. Cao et al., Dynamic linear calibration method for a wide range neutron flux monitor system in ITER. Nucl. Sci. Tech. **24**, 040402 (2013). doi:10.13538/j.1001-8042/nst.2013.04.002
7. D. Simeone, O. Hablot, V. Micalet et al., Contribution of recoil atoms to irradiation damage in absorber materials. J. Nucl. Mater. **246**, 206–214 (1997). doi:10.1016/S0022-3115(97)00092-5
8. G. Giorginis, V. Khriatchkov, The effect of particle leaking and its implications for measurements of the (n, α) reaction on light elements by using ionization chambers. Nucl. Instrum. Meth. A **538**, 550–558 (2005). doi:10.1016/j.nima.2004.08.106
9. D. Simeone, X. Deschanels, D. Gosset et al., Nuclear microprobe analysis of ^{7}Li profile induced in $HfB_2$by a neutron irradiation. J. Nucl. Mater. **297**, 244–250 (2001). doi:10.1016/S0022-3115(01)00644-4
10. G. Giorginis, V. Khryachkov, The cross-section of the ^{10}B (n, α) ^{7}Li reaction measured in the MeV energy range. Nucl. Instrum. Meth. A **562**, 737–740 (2006). doi:10.1016/j.nima.2006.02.035
11. G. Zhang, L. Guo, R. Cao et al., Cross-section measurement for the ^{10}B (n, α) ^{7}Li reaction at 4.0 and 5.0 MeV. Appl. Radiat. Isot. **66**, 1427–1430 (2008). doi:10.1016/j.apradiso.2007.07.035
12. Online, Available: http://geant4.cern.ch/
13. W.Z. Xu, Y.F. Liu, Z.Q. Tan et al., Geant4 simulation of plastic scintillators for a prototype μSR spectrometer. Nucl. Sci. Tech. **24**, 040401 (2013). doi:10.13538/j.1001-8042/nst.2013.04.011
14. X. Qin, R. Zhou, J.F. Han et al., GEANT4 simulation of the characteristic gamma-ray spectrum of TNT under soil induced by DT neutrons. Nucl. Sci. Tech. **26**, 010501 (2015). doi:10.13538/j.1001-8042/nst.26.010501
15. M.M. Nasseri, Q.L. Ma, Z.J. Yin et al., Monte-Carlo simulation for determining SNR and DQE of linear array plastic scintilating fiber. Nucl. Sci. Tech. **15**(5), 304–307 (2004)
16. M.M. Nasseri, Q.L. Ma, Z.J. Yin et al., Monte-Carlo simulation to determine detector efficiency of plastic scintillating fiber. Nucl. Sci. Tech. **15**(5), 308–311 (2004)
17. M.M. Nasseri, Q.L. Ma, Z.J. Yin, Image quality evaluation of linear plastic scintillating fiber array detector for X-ray imaging. Nucl. Sci. Tech. **15**(5), 255, 361–364 (2004)